npj | climate and atmospheric science

www.nature.com/npjclimatsci

ARTICLE OPEN

Check for updates

A future of extreme precipitation and droughts in the Peruvian Andes

Emily R. Potter[1,2,3✉], Catriona L. Fyffe[4], Andrew Orr[2], Duncan J. Quincey[1], Andrew N. Ross[5], Sally Rangecroft[6,7], Katy Medina[8,9], Helen Burns[5], Alan Llacza[10], Gerardo Jacome[10], Robert Å. Hellström[11], Joshua Castro[12], Alejo Cochachin[13,15], Nilton Montoya[12], Edwin Loarte[8,9] and Francesca Pellicciotti[4,14]

Runoff from glacierised Andean river basins is essential for sustaining the livelihoods of millions of people. By running a high-resolution climate model over the two most glacierised regions of Peru we unravel past climatic trends in precipitation and temperature. Future changes are determined from an ensemble of statistically downscaled global climate models. Projections under the high emissions scenario suggest substantial increases in temperature of 3.6 °C and 4.1 °C in the two regions, accompanied by a 12% precipitation increase by the late 21st century. Crucially, significant increases in precipitation extremes (around 75% for total precipitation on very wet days) occur together with an intensification of meteorological droughts caused by increased evapotranspiration. Despite higher precipitation, glacier mass losses are enhanced under both the highest emission and stabilization emission scenarios. Our modelling provides a new projection of combined and contrasting risks, in a region already experiencing rapid environmental change.

npj Climate and Atmospheric Science (2023)6:96 ; https://doi.org/10.1038/s41612-023-00409-z

INTRODUCTION

Mountain water resources in the tropical Andes sustain both rural and urban water supplies, irrigated agriculture, hydropower generation and fragile high-elevation ecosystems[1–3]. Most precipitation falls in the wet season between December and March, with glacier meltwater an important water source during the dry season (May to September), and especially during droughts[2,3]. Seventy percent of the world's tropical glaciers are in the Peruvian Andes, with most Peruvian glaciers concentrated in the Cordillera Blanca in northern Peru and the Cordilleras Vilcanota-Urubamba in southern Peru[4]. Both regions have undergone considerable glacier recession in recent decades[5–7], exacerbating water scarcity and conflicts around water allocation[1,8]. Rising temperatures have driven increases in freezing level height and snowline altitude[9–12], but the climate that is driving these dramatic changes remains poorly understood. Precipitation patterns in time and space remain uncertain, with some indication of increasing precipitation in the Cordillera Blanca, but not in the Cordillera Vilcanota-Urubamba[9,11,13,14].

Future projections based on global CMIP5 (Coupled Model Intercomparison Project version 5) models[15] suggest substantial temperature rises over the tropical Andes (of +1 °C to +5 °C) by 2100[16], and warming of +4.3 °C in the Vilcanota-Urubamba[17], and over +5 °C for the Quelccaya Ice Cap[18] under the highest emissions scenario, representative concentration pathway (RCP) 8.5 by 2100. These increases would likely lead to the disappearance of a large proportion of the region's glaciers[19]. Large-scale studies over South America suggest an increase in future precipitation in the wet season in the Peruvian Andes, based on CMIP6 models[20]. Few studies have investigated future precipitation in these two regions in detail, and none goes beyond 2030 for the Cordillera Blanca[21]. Notably, the few works in the Vilcanota-Urubamba region do not agree on the sign of precipitation change, with projections of both increases and decreases[22–24].

Populations in the Peruvian Andes are highly vulnerable to extreme weather events[25,26] and are at risk from both water scarcity and flooding[2,3]. Extremes such as heat waves and heavy precipitation are expected to increase in North-Western South America, based on global analysis using CMIP6 models[27]. To the best of our knowledge, there is no research on future heavy precipitation extremes directly in these two regions, and preliminary evidence from southern Peru suggests strong spatial variability in extreme climate indices in the recent past[13]. In a small region of the northern Andes, long-term extreme wet periods have increased more than meteorological droughts recently[26], but large-scale global climate model projections suggest most of the west coast of South America will experience an increase in droughts driven by evapotranspiration[28].

To determine precipitation and temperature in the recent past we run the Weather Research and Forecasting (WRF) model over the upper Rio Santa basin (in the Cordillera Blanca, hereafter referred to as Rio Santa), and the Vilcanota-Urubamba basin (Fig. 1a) from 1980 to 2018 at high spatial resolution (4 km). We correct the output for systematic biases in precipitation and temperature using weather station data. To determine future changes in temperature and precipitation, we statistically downscale precipitation and temperature from an ensemble of 30 CMIP5 models[29,30], with the bias-corrected WRF dataset used as the historical truth. To date, there have been no attempts to

[1]School of Geography, University of Leeds, Leeds, UK. [2]British Antarctic Survey, Cambridge, UK. [3]Department of Atmospheric and Cryospheric Sciences, University of Innsbruck, Innsbruck, Austria. [4]Engineering and Environment, Northumbria University, Newcastle-Upon-Tyne, UK. [5]School of Earth and Environment, University of Leeds, Leeds, UK. [6]School of Geography, College of Life and Environmental Sciences, University of Exeter, Exeter, UK. [7]School of Geography, Earth and Environmental Sciences, University of Plymouth, Plymouth, UK. [8]Instituto Nacional de Investigación de Glaciares y Ecosistemas de Montaña, Huaraz, Peru. [9]Santiago Antúnez de Mayolo National University, Huaraz, Peru. [10]Servicio Nacional de Meteorología e Hidrología del Perú, Lima, Peru. [11]Bridgewater State University, Bridgewater, Massachusetts, USA. [12]Universidad Nacional de San Antonio Abad del Cusco, Cusco, Peru. [13]Autoridad Nacional del Agua, Huaraz, Peru. [14]Swiss Federal Institute for Forest, Snow and Landscape Research, Zürich, Switzerland. [15]Deceased: Alejo Cochachin. ✉email: emily.potter@sheffield.ac.uk

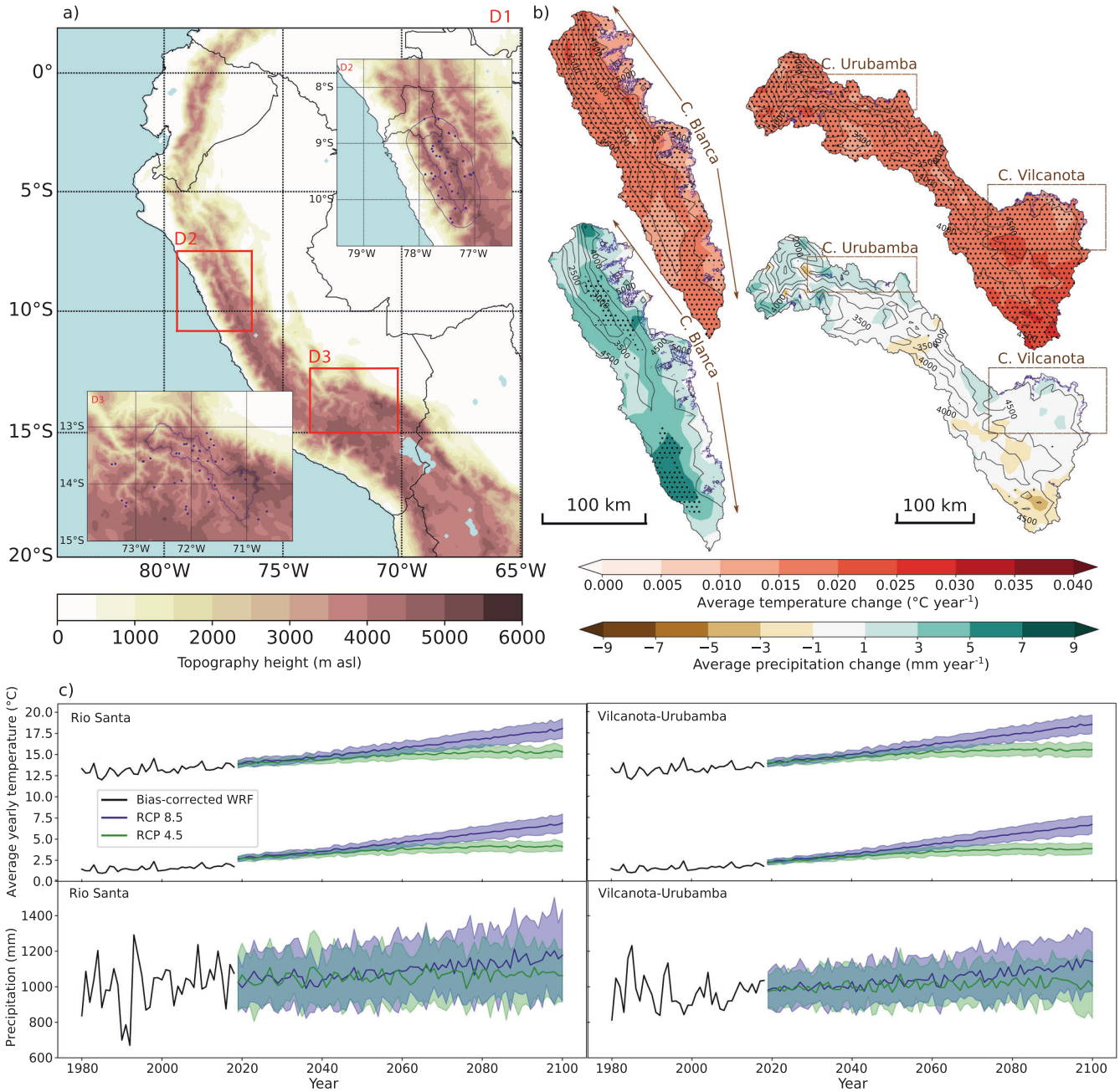

Fig. 1 Past and future trends in temperature and precipitation in the Rio Santa and Vilcanota-Urubamba basins. a The three WRF model domains (D1-D3) used for the 1980 to 2018 hindcast. The outer domain, D1, covers all of Peru at 12 km resolution. D2 and D3 show the inner domains at 4 km resolution, covering the Rio Santa basin and the Vilcanota-Urubamba basin, respectively. The two river basins are outlined in black, with the upper Rio Santa and 30 km boundary from which station data were used are outlined in blue. The terrain height is shown as filled contours, the ocean and other water bodies are shown in blue, and all stations used in the bias-correction are shown as blue dots. **b** The 1980-2018 annual trends in temperature (top; °C year^{-1}) and precipitation (bottom; mm year^{-1}) from the bias-corrected WRF hindcast, shown spatially for the upper Rio Santa (referred to as 'Rio Santa' in the text and hereafter) (left) and Vilcanota-Urubamba (right), with stippling indicating areas of significant trend and black contours showing elevation in 500 m intervals. The location of the Cordillera Blanca is shown with brown arrows, and the Cordilleras Urubamba and Vilcanota are marked by brown boxes. The outlines of the glaciers are shown in blue. **c** Timeseries of the basin-averaged recent past (1980-2018) and future (2019–2100) annual-averaged minimum and maximum daily temperature (top; °C) and precipitation (bottom; mm) are shown for the Rio Santa (left) and Vilcanota-Urubamba (right). Black lines show the basin-averaged values from the bias-corrected WRF hindcast. Blue lines show the mean of all statistically downscaled CMIP5 models for the RCP8.5 scenario, and green lines show the RCP4.5 scenario. Shading indicates one standard deviation from the mean (across the 30 statistically downscaled CMIP5 models).

downscale a large ensemble of global climate models for either the Rio Santa or the Vilcanota-Urubamba basins. We use these datasets to analyse past (1980–2018) and future (2019–2100) trends in temperature and precipitation. Future changes to daily extremes are analysed using six Expert Team on Climate Change Detection and Indices (ETCCDI) and future changes in meteorological droughts are determined using the Standardized Precipitation and Standardized Precipitation-Evapotranspiration

Indices (SPI and SPEI) for both the high (RCP8.5) and stabilization (RCP4.5) greenhouse gas emissions scenarios. All future changes are determined using the 30 statistically downscaled CMIP5 models, and compared to the control period 1980–2018 from the WRF hindcast.

RESULTS AND DISCUSSION

A complex picture of past climate trends

From 1980 to 2018, 2 m air temperature from the bias-corrected WRF data shows a basin-averaged increase of 0.016 °C year^{-1} in the Rio Santa and 0.018 °C year^{-1} in the Vilcanota-Urubamba (Fig. 1b), with statistical significance over most areas. These values are in-line with recent trends over Peru[10]. The high-resolution WRF data, however, allows us to determine spatial trends in new detail, and we find that over the higher elevation areas of the Rio Santa, the temperature rise has been smaller than in the lower areas, and is not statistically significant (Fig. 1b). In the Vilcanota-Urubamba, there is ubiquitous and statistically significant warming (Fig. 1b). From September to February, the Urubamba region in the north has warmed at a faster rate than the Vilcanota region in the south-east (Supplementary discussion section 1.1 and Supplementary Fig. 1). This is likely to have contributed to the increased glacier decline in the Urubamba region compared to the Vilcanota in recent decades[31].

Precipitation increased over the Rio Santa by an average of 3.1 mm year^{-1} between 1980 and 2018 according to the bias-corrected WRF data, but the increases are only statistically significant over the south-west of the region (Fig. 1b). In the Vilcanota-Urubamba, precipitation has increased in the north of the basin, around the Cordillera Urubamba, and decreased in the south, but with no statistically significant trends when considered annually (Fig. 1b). In September-October-November (SON) there is statistically significant drying over some glacierised regions of both the Rio Santa and the Cordillera Urubamba, as well as in the south of the Vilcanota-Urubamba Basin (Supplementary discussion section 1.1 and Supplementary Fig. 1). The combination of a particularly large increase in temperature and a reduction in precipitation in September-October-November, which is the end of the dry season (Supplementary discussion section 1.1 and Supplementary Fig. 1), is likely to have been particularly damaging to the glaciers, which have the lowest snow cover and therefore lower albedos at this time. A drying trend during the start of the wet season may also lead to agricultural changes, as September rainfall is important for crop sowing[32].

There is good confidence in the past changes presented, as the correlation coefficients between the WRF data and the observations are high. They average 0.83 for the stations around the Rio Santa and 0.85 for the Vilcanota-Urubamba for monthly precipitation, and 0.78 (0.69) for the Rio Santa and 0.92 (0.74) for the Vilcanota-Urubamba for minimum (maximum) daily temperature, averaged monthly. The bias-correction substantially reduces the average root mean square error between the WRF data and the observations. This comparison, and a comparison with other gridded temperature and precipitation products, is shown in Supplementary methods section 2.1.1 and Supplementary Fig. 3.

A warmer, wetter future with increasing glacier melt

Both the Rio Santa and the Vilcanota-Urubamba regions will experience substantial warming until 2100 under both the RCP8.5 and RCP4.5 emissions scenarios based on the output from the statistically downscaled CMIP5 models, but with a clear divergence in trajectories between scenarios (Fig. 1c). By the late 21st century (2062-2100), maximum daily temperature increases of 3.6 °C and 4.1 °C in the Rio Santa and Vilcanota-Urubamba are projected under RCP8.5, compared to the recent past control period (1980–2018) (increases are of 1.9 °C and 2.2 °C under RCP4.5 (Table 1)). The rises in the minimum daily temperature are similar to those in the maximum daily temperature. The maximum and minimum daily temperature increases are statistically significant across all statistically downscaled CIMP5 models in both time periods and RCP scenarios (Table 1).

Annual precipitation will increase by 12.1% (123 mm year^{-1}) in the Rio Santa and 12.2% (118 mm year^{-1}) in the Vilcanota-Urubamba by the late 21st century under RCP8.5, and 5.8% (59 mm year^{-1}) in the Rio Santa and 5.3% (52 mm year^{-1}) in the Vilcanota-Urubamba by the late 21st century under RCP4.5 (Table 1, Fig. 1c). There is variation between the statistically downscaled CMIP5 models, with a standard deviation of 11% in the Rio Santa and 9.3% in the Vilcanota-Urubamba, under RCP8.5 by the late 21st century.

Importantly, the increasing precipitation shown here for the Vilcanota-Urubamba is in contrast to ref. [24], who suggested that increasing westerly winds at 200 hPa are likely to cause a reduction in precipitation over the Central Andes (including the Vilcanota-Urubamba region). While the correlation between high-altitude westerly winds and precipitation is well established for the present[24,33,34], regional climate models over South America suggest mixed trends over the Peruvian Andes in the future, with a rise in precipitation over most of the country[35], but with insufficient spatial resolution to determine trends for these two

Table 1. Statistically downscaled CMIP5 multi-model average mean (and standard deviation, in brackets) projected increases in maximum and minimum temperature (°C) and annual precipitation (%) in the mid- (2022–2060) and late- (2062–2100) 21st century for the Rio Santa and Vilcanota-Urubamba regions, compared to the control period (1980–2018).

	Variable	Rio Santa		Vilcanota-Urubamba	
		2022–2060	2062–2100	2022–2060	2062–2100
RCP4.5	Maximum daily temperature (°C)	1.2 (±0.3)	1.9 (±0.6)	1.4 (±0.3)	2.2 (±0.6)
	Minimum daily temperature (°C)	1.2 (±0.3)	2.0 (±0.5)	1.3 (±0.3)	2.1 (±0.6)
	Precipitation (%)	3.8 (±3.4)	5.8 (±6.3)	3.5 (±3.9)	5.3 (±6.5)
		25	*24*	*23*	*23*
RCP8.5	Maximum daily temperature (°C)	1.6 (±0.4)	3.6 (±0.8)	1.8 (±0.4)	4.1 (±0.8)
	Minimum daily temperature (°C)	1.6 (±0.3)	3.7 (±0.8)	1.7 (±0.3)	4.0 (±0.8)
	Precipitation (%)	4.5 (±5.4)	12.1 (±11.0)	4.7 (±4.8)	12.2 (±9.3)
		26	*27*	*28*	*28*

Numbers in italics denote the number of statistically downscaled CMIP5 models showing an increase in precipitation (of 30). All statistically downscaled CMIP5 models show an increase in the temperature variables.

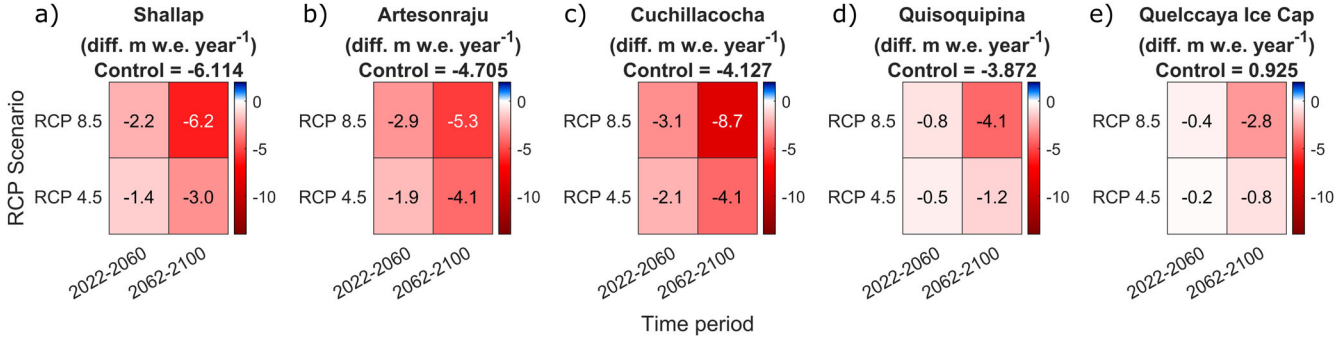

Fig. 2 Future glacier mass balance change. Change in mass balance rate (in metres water equivalent per year) due to the climatic changes projected in this manuscript at five on-glacier weather station sites in the two regions: the (**a**) Shallap (4790 m asl), (**b**) Artesonraju (4797 m asl), and (**c**) Cuchillacocha (4821 m asl) Glaciers in the Rio Santa region, and the (**d**) Quisoquipina Glacier (5180 m asl) and (**e**) Quelccaya Ice Cap (5650 m asl) in the Vilcanota-Urubamba region. Changes are shown for the mid- (2022–2060) and end- (2062–2100) 21st century for the RCP4.5 and RCP8.5 emissions scenarios, with the mass balance rate for the control period for each station (see ref. [36]) above each box. Note that the negative mass balances in the control period for Shallap, Artesonraju, Cuchillacocha and Quisoquipina imply that these stations are located in the ablation zone of the glaciers. These outputs are calculated in the same way as the sensitivity test method used in ref. [36].

regions. Here we show that almost all the statistically downscaled CMIP5 models project an increase in precipitation in both regions by the late 21st century, with over half showing a statistically significant increase (Table 1, Supplementary Tables 8, 9).

The projected changes in temperature and precipitation will have important consequences for glaciers and water resources. Using the future precipitation and temperature changes from the statistically downscaled CMIP5 models, we determine the potential effect on the glacier mass balance at the five on-glacier weather station sites (located in the Rio Santa and Vilcanota-Urubamba) studied in[36]. Under RCP8.5 by the late 21st century, the rate of mass loss more than doubles at all five sites, with the current accumulation found at the summit of Quelccaya Ice Cap in the Vilcanota-Urubamba, the highest site, changing to substantial mass loss (from +0.925 m we year^{-1} (metres water equivalent per year) to −1.875 m we year^{-1}) (Fig. 2). Under RCP4.5, the increase in mass loss is smaller at all glaciers, but in no future time period or RCP scenario are the increases in precipitation sufficient to prevent an increase in the rate of glacier mass loss (Supplementary discussion section 1.2, Supplementary Fig. 2 and ref. [36] for details). Increased glacier shrinkage can heighten the risk of GLOFs (glacier lake outburst floods), and will reduce runoff in the dry season, exacerbating current water scarcity[8,17].

The greatest uncertainty in the future projections is in the different trends from the CMIP5 models themselves, and arises from a combination of model uncertainty, emissions scenario uncertainty and internal variability[37]. However, the robustness in the sign of the change from the large ensemble of model projections used here indicates the consistency of these results. The statistical downscaling method used here, quantile delta mapping, is designed to preserve the original trends in the CMIP5 models at all quantiles[29], but correct the magnitude of temperature and precipitation, and the number of wet days, based on the bias-corrected WRF data. The choice of control period influences the magnitude of the future changes, but the increasing temperature and precipitation trends are consistent across all control periods tested (starting from 1950), see Supplementary methods section 2.2.1.

Amplified heavy precipitation and warm spells

A key finding of this work is that heavy precipitation will increase at a much higher rate than total precipitation (Fig. 3a–c). Average precipitation on wet days (calculated using the simple precipitation intensity index (SDII, see methods) and spatially averaged over the domains) shows a statistically significant increase in 23 of the 30 statistically downscaled CMIP5 models by the late 21st century under RCP8.5, with the median year in each period (averaged over all the statistically downscaled CMIP5 models) increasing from 6.3 mm day^{-1} in the control period to 7.1 mm day^{-1} between 2062 and 2100 in the Rio Santa annually, an increase of 12.7% (Fig. 3a). In the Vilcanota-Urubamba, 27 of the 30 statistically downscaled CMIP5 models show a statistically significant increase from 6.2 mm day^{-1} to 7.0 mm day^{-1}, an increase of 13.0% (Fig. 3a). No models show a statistically significant decrease in simple precipitation index in either region. Importantly, however, total precipitation falling on heavy precipitation days (95th percentile from the control period, (R95pTOT, see methods)) is projected to increase substantially more than average precipitation (Fig. 3c). These increases are largest under RCP8.5 in both regions, with precipitation under this scenario from very wet days in the median year by the late 21st century (276.0 and 262.7 mm in the Rio Santa and Vilcanota-Urubamba, respectively) about 75% higher than the median year amounts for the control period (158.4 and 149.0 mm). Under RCP4.5, these increases are about 30% by the late 21st century. The number of dry days in the year (and seasonally) does not show any substantial change in either region or scenario, with a maximum of 4 out of 30 models showing a statistically significant increase (Fig. 3b), indicating that these changes are due to increasing precipitation on wet days, rather than an increase in the number of wet days. All the precipitation indices show substantial interannual variability, with overlap between the two scenarios.

The monthly maximum temperatures (TX_x) will rise substantially, slightly over the average temperature increases (Table 1), from a median of 15.3 °C in the control period to 19.1 °C under RCP8.5 by the late 21st century in the Rio Santa, and from 15.6 °C to 19.8 °C in the Vilcanota-Urubamba (Fig. 3d). Rising temperatures lead to a large increase in warm days (calculated using the warm spell duration index (WSDI, see methods)), and a decrease in the number of frost days per year (Fig. 3e, f). The number of days per year within warm spells increases from 10.9 (5.7) in the Rio Santa (Vilcanota-Urubamba) in the control period to 171.0 (172.8) by the late 21st century under RCP4.5, and 287.8 (306.8) under RCP8.5, meaning that almost every day of the year is projected to be in the top 10% of 1980–2018 days, with consistency in sign across models. The median number of frost days per year (FD) is projected to reduce by around half, from 115.7 and 131.0 days (1980–2018) to 73.5 and 88.7 (64.0 and 79.4) days, under RCP4.5 (8.5) by mid-century (2022–2060), in the Rio Santa and Vilcanota-Urubamba, respectively (Fig. 3f). By the late 21st century, under RCP8.5, there will only be a handful of frost days per year, with a

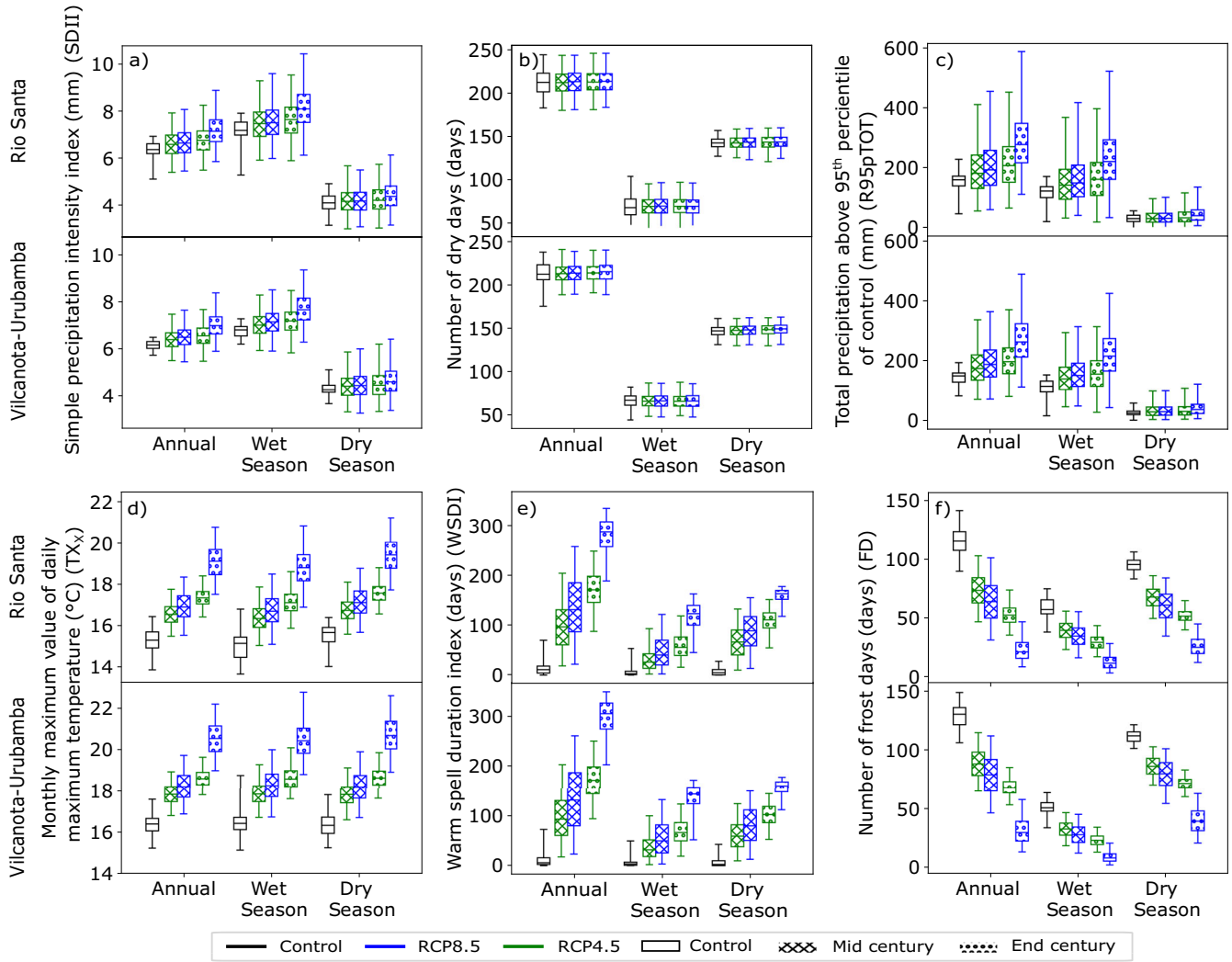

Fig. 3 Future change in temperature and precipitation climate indices. Box and whisker plots of basin-averaged precipitation and temperature ETCCDI (Expert Team on Climate Change Detection and Indices) for the Rio Santa (top in each pair) and Vilcanota-Urubamba (bottom of each pair) regions for the control period (1980–2018; black boxes), as well as the mid- (2022–2060; hatching) and end of- (2062–2100; dots) 21st century for RCP4.5 (green boxes) and RCP8.5 (blue boxes) emissions scenarios. Results are shown annually, as well as for wet (November to April) and dry (May to October) seasons. For the control period, the middle of the box shows median year from the bias-corrected WRF hindcast, the top (bottom) of the box shows the 75th (25th) quantiles, and the top (bottom) of the whisker shows the maximum (minimum) year. For the future period boxes, the multi-model mean is taken for each quantile from the statistically downscaled CMIP5 models. Panel (**a**) shows the average precipitation on wet days (SDII), (**b**) shows the number of dry days, (**c**) shows the total precipitation falling on days above the 95th quantile of the control period (R95pTOT), (**d**) shows the monthly maximum of daily maximum temperature (TX_x), (**e**) shows the warm spell duration index (i.e., days where at least six consecutive days fall above the 90th percentile of the control period) (WSDI), (**f**) shows the number of frost days (FD).

statistically significant decrease in all statistically downscaled CMIP5 models.

The increase in extreme precipitation is likely due to a shift in the distribution of precipitation intensity, such that a greater proportion of days are above the 95th quantile of the control period. In addition, although the Clausius-Clapeyron equation suggests an increase of approximately 7% in atmospheric water vapour for every 1 K of warming, precipitation has been shown to increase at a much smaller rate[38]. This is consistent with our results, which show precipitation increases of 12% for around 4 K of warming. However, extreme precipitation events, which are typically short-lived, are able to follow Clausius-Clapeyron scaling to its maximum extent. This implies, as is shown in these results, increases in heavy precipitation many times larger than the average precipitation increases.

Extreme rainfall is the most frequent cause of climatic natural hazards such as floods and landslides[39–41]. Andean farming communities also report an agricultural risk from heavy rains, which can wash away soil and destroy crops[32]. In addition to the effects of heavy precipitation, the decrease in frost days and increase in warm spells found in this study are likely to influence agricultural practices in these regions in the future. While the decrease in frost days may be beneficial to some crops grown in the Andes, others will either have to be sown at a different time of year, or replaced with different varieties[32,42–44].

Future droughts projected to increase due to evapotranspiration

Meteorological droughts in the two study regions are expected to increase in the future based on the Standardised Precipitation-Evapotranspiration Index (SPEI, see methods), i.e., when potential evapotranspiration is accounted for[45]. SPEI is projected to decrease (indicating a long-term drying trend) over both regions

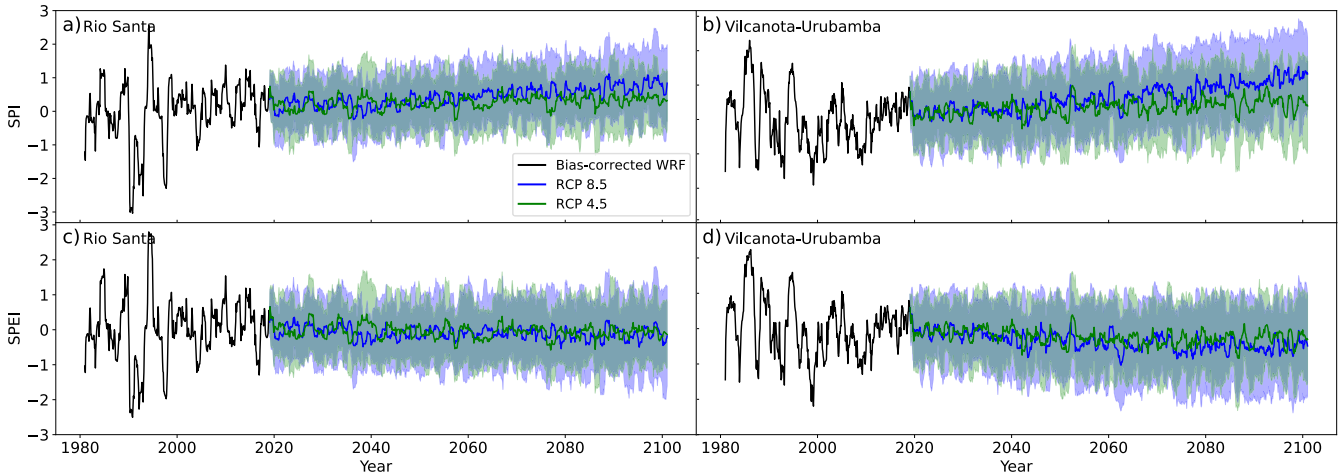

Fig. 4 Past and future drought indices. Timeseries of the basin-averaged recent past (1980–2018) and future (2019–2100) Standardised Precipitation Index (SPI; **a** and **b**) and Standardised Precipitation-Evapotranspiration Index (SPEI; **c** and **d**) for the Rio Santa (**a** and **c**) and Vilcanota-Urubamba (**b** and **d**) regions. The black lines show the values from the bias-corrected WRF hindcast. The blue lines show the mean of all statistically downscaled CMIP5 models for the RCP8.5 scenario, and the green lines show the RCP4.5 scenario. Shading indicates one standard deviation from the mean (across the 30 statistically downscaled CMIP5 models).

Table 2. Basin-averaged number of drought months for the Rio Santa and Vilcanota-Urubamba regions for the control period (1980–2018) and mid- (2022–2060) and late- (2062–2100) 21st century, based on values of the Standardised Precipitation Index (SPI) and Standardised Precipitation-Evapotranspiration Index (SPEI).

	Drought characteristics	Rio Santa			Vilcanota-Urubamba		
		1980–2018	2022–2060	2062–2100	1980–2018	2022–2060	2062–2100
SPI RCP4.5	Total number of drought months	86.4	67.2	63.8	114.9	88.2	78.3
	Number of CMIP5 models with drought months > control period	N/A	9	11	N/A	10	6
SPEI RCP4.5	Total number of drought months	96.1	110.8	134.6	110.2	145.8	172.3
	Number of CMIP5 models with drought months > control period	N/A	16	20	N/A	21	24
SPI RCP8.5	Total number of drought months	86.4	70.3	46.6	114.9	84.7	56.1
	Number of CMIP5 models with drought months > control period	N/A	9	5	N/A	8	4
SPEI RCP8.5	Total number of drought months	96.1	129.8	174.0	110.2	157.9	211.3
	Number of CMIP5 models with drought months > control period	N/A	19	23	N/A	21	24

The SPI and SPEI indices are calculated for the previous 12 months (SPI/SPEI-12), and therefore the first month in the first year of each period is December. As such, all drought months are out of a total possible 457 months (from 1980–2018, 2022–2060 or 2062–2100). Results for the control period (future) are based on the bias-corrected WRF hindcast (mean of the downscaled ensemble of CMIP5 models). Also shown are the number of statistically downscaled CMIP5 models (out of 30) with more drought months for the future periods than the control period.

and both RCP scenarios (Fig. 4c, d). The rising future temperatures discussed above (Fig. 1, Table 1) are reflected in a considerable increase in the number of drought months, by over 50% from 110.2 out of 457 months in the control period 1980–2018 to 172.3 out of 457 months by the late 21st century 2062-2100, in the Vilcanota-Urubamba under RCP4.5. In the Rio Santa, the increase is just under 50%, from 96.1 to 134.6 months (Table 2). Under RCP8.5, the average number of drought months will almost double in both regions, to 174.0 in the Rio Santa and 211.3 in the Vilcanota-Urubamba by the late 21st century. These changes are seen across most of the statistically downscaled CMIP5 models, with around two-thirds or more of the models projecting increases in drought months under both RCP scenarios in both regions by the late 21st century (Table 2).

Importantly, this increase in droughts is not apparent when analysing droughts from precipitation only using the Standardised Precipitation Index (SPI, see methods)[46], which shows increases in both regions and for both RCPs (Fig. 4a, b), i.e. reduced meteorological drought events, reflecting the increasing trends in average precipitation (Fig. 1). Accordingly, the spatially-averaged number of drought months calculated using SPI is predicted to decrease considerably in both regions, with most statistically downscaled CMIP5 models showing a decrease in both regions by the late 21st century under RCP8.5 (Table 2). While using potential evapotranspiration can lead to an overestimation of future drought compared to actual evapotranspiration[47,48], these contrasting results highlight that evapotranspiration plays a particularly important role in this part of the Andes and is essential in projections of future drought.

Meteorological drought is considered the leading cause of drought[26], and water scarcity is already reported by local populations in both the Rio Santa and Vilcanota-Urubamba basins[49]. There is an increase in the inter-annual variability of precipitation in 22 of the statistically downscaled CMIP5 models for the Rio Santa and 25 statistically downscaled CMIP5 models for the Vilcanota-Urubamba, by the late 21st century under RCP8.5 (Supplementary tables 8 and 9). The greater variation in precipitation, along with intensifying evapotranspiration, is likely to increase both very wet and very dry months, and may be

caused by increases in El Niño-Southern Oscillation (ENSO) variability[50].

It should be noted that here potential evapotranspiration is estimated using a relatively simple formula, and that estimated potential evapotranspiration can be greater than actual evapotranspiration during periods of low precipitation. A full hydrological model would be needed to project future hydrological droughts.

Which future for the Andes?

Here we find a complex picture of past and future changes in the Andes of Peru, with the projected joint occurrence of both increased droughts and extreme precipitation. Further work is now needed for hydrological and societal modelling to determine the impact of meteorological droughts on hydrological changes, livelihoods, agriculture and hydroelectric power, and to provide scenarios of changes in the combined physical and socio-economic systems that are able to account for the very high variability in climatic changes identified in this study.

Given the likely glacier mass loss driven by these climate changes, the importance of glacier melt for dry season runoff[3] and our predicted increase in drought conditions, these two Andean regions are likely to see enhanced dry season water stress in the future. This would have impacts on agriculture, including the irrigated export agriculture schemes on the Pacific coast fed by runoff from the Rio Santa[2] and the farmers in the Andean highlands[44,51], as well as ecological impacts (e.g. on wetland habitats[52]). Increased extreme precipitation may partly replenish groundwater supplies, which are crucial for maintaining river discharge in the dry season, but it would likely also lead to an increase in flooding, with associated economic and human consequences[53].

The clear divergence between the two RCP scenarios reiterates the necessity of reducing global emissions. In addition, these results point to the need for urgent action to mitigate the future effects of climate change[53]. Early warning systems have proved effective for mitigating against the impacts of floods and landslides[54,55]. Diversifying water sources and improving both infrastructure and water governance can increase water access in the dry season[56], and crop diversification may improve farming yields with climate change[57,58]. These adaptations have been shown to have much higher success when planned and developed with local populations, integrating indigenous knowledge into the adaptation process[59,60]. This work provides the first evidence base to inform novel adaptation and mitigation measures and inspire a new generation of land surface modelling to disentangle the consequences of the complex climatic changes we have identified.

METHODS

Historical regional climate model

The WRF model version 3.8.1[61] is run with an outer domain of 12 km resolution covering Peru, and two 4 km inner domains; D2 over the Rio Santa and D3 over the Vilcanota-Urubamba (Fig. 1), with hourly temporal output (details of the WRF setup in Supplementary Table 1 and ref. [36]). The model is driven with data from ERA5 at the boundaries[62]. Regional climate models have been found to accurately represent the spatio-temporal patterns in precipitaotn and temperature in the Andes[63,64], and the WRF output is bias-corrected using present-day observations to reduce systematic biases.

Total daily precipitation and minimum and maximum daily air temperature at 2 m were compared to and bias-corrected against observations, from 35 (35) precipitation and 26 (34) temperature stations around the Rio Santa (Vilcanota-Urubamba). Station data originates from Servicio Nacional de Meteorología e Hidrología del Perú (SENAMHI)[65], CIAD de la Universidad Nacional Santiago Antunez de Mayolo (UNASAM), Área de Evaluación de Glaciares y Lagunas de la Autoridad Nacional del Agua (ANA), Universidad Nacional de San Antonio Abad del Cusco (UNSAAC), and Compañia Minera Antamina S.A., de Perú. All stations have some data in the years between 1980 and 2018, and the data were cleaned before use (see ref. [36] for details). Locations of the observational stations are shown in Fig. 1a D2 and D3. Full details of the in-situ weather stations can be found in Supplementary Tables 2 and 3. The precipitation and temperature observations were used to correct the magnitude of the daily temperature output, and the number of wet days and magnitude of the precipitation output (see Supplementary methods, section 2.1).

Statistical downscaling of CMIP5 models

To determine regional changes in the Rio Santa and Vilcanota basins over the 21st century, 30 CMIP5 model projections were statistically downscaled using the bias-corrected WRF dataset in place of observations (Supplementary Table 7 gives details of the CMIP5 models used). The statistical downscaling was carried out for RCP4.5 and RCP8.5, based on the quantile delta mapping method described by Cannon et al. [29]. This method preserves the large-scale trends from the CMIP5 models at each quantile (i.e. the trends in both the median and the extremes are preserved), while adjusting the number of wet days and the magnitude of precipitation and temperature based on the values from 1980 to 2018. Further details are available in Supplementary methods section 2.2. Statistical significance for the changes shown in Table 1 was assessed using a bootstrap method[66].

Climate change indices

Six of the Expert Team on Climate Change Detection and Indicies (ETCCDI) climate indices[67] were calculated in this study: the simple precipitation intensity index describing the total annual precipitation on wet days; the annual total precipitation falling on days where precipitation is above the 95th percentile of the 1980-2018 period; the number of dry days (precipitation under 1 mm) in a year (a variation on 'continuous dry days' given in[67]); the annual average monthly maximum temperature; the warm spell duration index describing the annual count of days with at least 6 consecutive days above the 90th percentile of daily maximum temperature from 1980-2018; and the number of frost days (minimum daily temperature below 0 °C). Indices were calculated based on the python package xclim,[68], and statistical significance was assessed using a bootstrap method[66].

Drought indices

The standard precipitation index (SPI) transforms the probability density function of precipitation to a standardised normal distribution, such that a value of −1 represents one standard deviation below (drier than) the mean[46]. To calculate the Standard Precipitation-Evapotranspiration Index (SPEI), potential evapotranspiration is estimated using the Hargreaves equation[69], estimating the extra-terrestrial solar radiation from the latitude and day of year (calculated using the python software package Pyeto). The values of precipitation minus potential evapotranspiration are then transformed to a standardized normal distribution. The SPI and SPEI indices are calculated per month, rolling over the previous 12 months (SPI-12 and SPEI-12)[45]. Note that as the SPI and SPEI indices for a month are based on the previous 12 months, the first control period value is for December 1980. December is taken as the starting month for the mid-century and end-century in the drought calculations to keep the time periods consistent in length. We characterise a drought event as one where the index falls below one negative standard deviation for two consecutive months, which ends when the index turns positive[28,70]. Note that

here we use 1980-2018 as the reference period, rather than the entire timeseries used by[28], in order to determine the impact of droughts without adaptation. Further information is given in Supplementary methods section 2.3.

Glacier change

The changes in future precipitation and temperature were calculated at each of five on-glacier weather stations sites in the two regions, to project the change in the mass balance of the glaciers at these sites. At each site we ran the energy-balance melt model component of Tethys-Chloris at the point scale (using the same set-up as in ref. [36] for the climate sensitivity experiments), both with no change (control) and applying the average modelled changes in air temperature and precipitation under RCP scenarios 4.5 and 8.5, and for the mid- and end-of century projections detailed in this manuscript at each station. The vapour pressure and dew point temperature were recalculated based on the changes to the air temperature, but no other changes were made to other input variables.

Inclusion and ethics statement

This research was funded jointly between Peruvian and UK funding agencies, and roles and responsibilities were agreed amongst collaborators before the start of the project. This manuscript is a collaboration between Peruvian and UK researchers, as well as international partners, and all authors were involved throughout the manuscript process. Peruvian research and reports have been cited where appropriate for this study.

DATA AVAILABILITY

The data used in this article is all available at the Polar Data Centre. The raw WRF output is available at https://doi.org/10.5285/7F3E4CFC-B75B-4758-85FC-58634BD7B1D1. The bias-corrected data are available at https://doi.org/10.5285/2CF25580-9B79-440F-8505-6230DD377877. The future temperature, precipitation and evapotranspiration from the statistically downscaled CMIP5 models are available at https://doi.org/10.5285/67CEB7C8-218C-46E1-9927-CFEF2DD95526, and the future ETCCDI datasets are available at https://doi.org/10.5285/B56D30E8-EDAA-4225-96D7-FCC689E930C7.

CODE AVAILABILITY

The code used for the bias correction and statistical downscaling are available at https://github.com/Empott/Bias-correction_and_CMIP_downscaling.

Received: 16 August 2022; Accepted: 26 June 2023;
Published online: 20 July 2023

REFERENCES

1. Vergara, W. et al. Economic impacts of rapid glacier retreat in the Andes. *Eos, Trans. Am. Geophys. Union* **88**, 261–264 (2007).
2. Drenkhan, F., Carey, M., Huggel, C., Seidel, J. & Oré, M. T. The changing water cycle: climatic and socioeconomic drivers of water-related changes in the Andes of Peru. *Wiley Interdiscip. Rev. Water* **2**, 715–733 (2015).
3. Buytaert, W. et al. Glacial melt content of water use in the tropical Andes. *Environ. Res. Lett.* **12**, 114014 (2017).
4. Morales Arnao, B. & Hastenrath, S. Glaciers of South America: Glaciers of Peru. Tech. Rep. 1386I, US Geological Survey professional paper (1998).
5. Gurgiser, W., Marzeion, B., Nicholson, L., Ortner, M. & Kaser, G. Modeling energy and mass balance of Shallap Glacier, Peru. *Cryosphere* **7**, 1787–1802 (2013).
6. Hanshaw, M. N. & Bookhagen, B. Glacial areas, lake areas, and snow lines from 1975 to 2012: status of the Cordillera Vilcanota, including the Quelccaya Ice Cap, northern central Andes, Peru. *The Cryosphere* **8**, 359–376 (2014).
7. Suarez, W. et al. Balance enérgetico neto (2012-2014) y evolución temporal del nevado Quisoquipina en la región de Cusco (1990-2010). *Revista Peruana Geo-Atmosférica* **4**, 80–92 (2015).
8. Motschmann, A. et al. Losses and damages connected to glacier retreat in the Cordillera Blanca, Peru. *Clim. Chang.* **162**, 837–858 (2020).
9. Salzmann, N. et al. Glacier changes and climate trends derived from multiple sources in the data scarce Cordillera Vilcanota region, southern Peruvian Andes. *Cryosphere* **7**, 103–118 (2013).
10. Vicente-Serrano, S. M. et al. Recent changes in monthly surface air temperature over Peru, 1964–2014. *Int. J. Climatol.* **38**, 283–306 (2018).
11. Schauwecker, S. et al. Climate trends and glacier retreat in the Cordillera Blanca, Peru, revisited. *Global Planet. Chang.* **119**, 85–97 (2014).
12. Veettil, B. K., Wang, S., Bremer, U. F., de Souza, S. F. & Simões, J. C. Recent trends in annual snowline variations in the northern wet outer tropics: case studies from southern Cordillera Blanca, Peru. *Theor. Appl. Climatol.* **129**, 213–227 (2017).
13. Heidinger, H., Carvalho, L., Jones, C., Posadas, A. & Quiroz, R. A new assessment in total and extreme rainfall trends over central and southern Peruvian Andes during 1965–2010. *Int. J. Climatol.* **38**, e998–e1015 (2018).
14. Hänchen, L. et al. Widespread greening suggests increased dry-season plant water availability in the Rio Santa valley, Peruvian Andes. *Earth Syst. Dyn.* **13**, 595–611 (2022).
15. Taylor, K. E., Stouffer, R. J. & Meehl, G. A. An overview of CMIP5 and the experiment design. *Bull. Am. Meteorol. Soc.* **93**, 485–498 (2012).
16. Vuille, M. et al. Rapid decline of snow and ice in the tropical Andes–Impacts, uncertainties and challenges ahead. *Earth-Sci. Rev.* **176**, 195–213 (2018).
17. Drenkhan, F., Guardamino, L., Huggel, C. & Frey, H. Current and future glacier and lake assessment in the deglaciating Vilcanota-Urubamba basin, Peruvian Andes. *Global Planet. Chang.* **169**, 105–118 (2018).
18. Yarleque, C. et al. Projections of the future disappearance of the Quelccaya Ice Cap in the Central Andes. *Sci. Rep.* **8**, 1–11 (2018).
19. Schauwecker, S. et al. The freezing level in the tropical Andes, Peru: An indicator for present and future glacier extents. *J. Geophys. Res. Atmos.* **122**, 5172–5189 (2017).
20. Almazroui, M. et al. Assessment of CMIP6 performance and projected temperature and precipitation changes over South America. *Earth Syst. Environ.* **5**, 155–183 (2021).
21. Obregón, G. et al. Escenarios climáticos en la cuenca del Río Santa para el año 2030: resumen técnico. Tech. Rep., Servicio Nacional de Meteorología e Hidrología del Perú (2009).
22. Ávalos, G., Díaz, A., Oria, C., Metzger Terrazas, L. & Acuña, D. Escenarios de cambio climático en la cuenca del Río Urubamba para el año 2100: resumen técnico. Tech. Rep., Servicio Nacional de Meteorología e Hidrología del Perú (2010).
23. Marengo, J. A. et al. Climate change: evidence and future scenarios for the Andean region. Tech. Rep., Climate change and biodiversity in the tropical Andes. IAI-SCOPE-UNESCO, Paris, France (2011).
24. Neukom, R. et al. Facing unprecedented drying of the Central Andes? Precipitation variability over the period AD 1000–2100. *Environ. Res. Lett.* **10**, 084017 (2015).
25. Poveda, G. et al. High impact weather events in the Andes. *Front. Earth Sci.* **8**, 162 (2020).
26. Rascón, J., Gosgot Angeles, W., Quiñones Huatangari, L., Oliva, M. & Barrena Gurbillón, M. Á. Dry and wet events in Andean populations of Northern Peru: A case study of Chachapoyas, Peru. *Front. Environ. Sci.* **9**, 54 (2021).
27. Almazroui, M. et al. Projected changes in climate extremes using CMIP6 simulations over SREX regions. *Earth Syst. Environ.* **5**, 481–497 (2021).
28. Spinoni, J. et al. Future global meteorological drought hot spots: a study based on cordex data. *J. Climate* **33**, 3635–3661 (2020).
29. Cannon, A. J., Sobie, S. R. & Murdock, T. Q. Bias correction of GCM precipitation by quantile mapping: how well do methods preserve changes in quantiles and extremes? *J. Climate* **28**, 6938–6959 (2015).
30. Lutz, A. F. et al. South Asian river basins in a 1.5 C warmer world. *Reg. Environ. Chang.* **19**, 833–847 (2019).
31. Taylor, L. et al. Multi-decadal glacier area and mass balance change in the Southern Peruvian Andes. *Front. Earth Sci.* **10**, 863933 (2022).
32. Gurgiser, W. et al. Comparing peasants' perceptions of precipitation change with precipitation records in the tropical Callejón de Huaylas, Peru. *Earth System Dyn.* **7**, 499–515 (2016).
33. Minvielle, M. & Garreaud, R. D. Projecting rainfall changes over the South American Altiplano. *J. Climate* **24**, 4577–4583 (2011).
34. Thibeault, J., Seth, A. & Wang, G. Mechanisms of summertime precipitation variability in the Bolivian Altiplano: present and future. *Int. J. Climatol.* **32**, 2033–2041 (2012).
35. Llopart, M., Simões Reboita, M. & Porfírio da Rocha, R. Assessment of multi-model climate projections of water resources over South America CORDEX domain. *Climate Dyn.* **54**, 99–116 (2020).
36. Fyffe, C. L. et al. The energy and mass balance of Peruvian glaciers. *J. Geophys. Res. Atmos.* **126**, e2021JD034911 (2021).

37. Hawkins, E. & Sutton, R. The potential to narrow uncertainty in regional climate predictions. *Bull. Am. Meteorol. Soc.* **90**, 1095–1108 (2009).
38. Held, I. M. & Soden, B. J. Robust responses of the hydrological cycle to global warming. *J. Climate* **19**, 5686–5699 (2006).
39. Vilímek, V., Hanzlík, J., Sládek, I., Šandov, M. & Santillán, N. The share of landslides in the occurrence of natural hazards and the significance of El Niño in the Cordillera Blanca and Cordillera Negra Mountains, Peru. *Landslides: Global Risk Preparedness*133–148 (2013).
40. Klimeš, J. & Vilímek, V. A catastrophic landslide near Rampac Grande in the Cordillera Negra, northern Peru. *Landslides* **8**, 309–320 (2011).
41. Engel, Z., Česák, J. & Escobar, V. R. Rainfall-related debris flows in Carhuacocha Valley, Cordillera Huayhuash, Peru. *Landslides* **8**, 269–278 (2011).
42. Tapia, M. E., Fries, A. M., Mazar, I. & Rosell, C. Guía de campo de los cultivos andinos (Field Guide to Andean Crops). Tech. Rep., FAO, ANPE-PERÚ (2007).
43. Sanabria, J., Calanca, P., Alarcón, C. & Canchari, G. Potential impacts of early twenty-first century changes in temperature and precipitation on rainfed annual crops in the Central Andes of Peru. *Reg. Environ. Change* **14**, 1533–1548 (2014).
44. Postigo, J. C. Perception and resilience of Andean populations facing climate change. *J. Ethnobiol.* **34**, 383–400 (2014).
45. Vicente-Serrano, S. M., Beguería, S. & López-Moreno, J. I. A multiscalar drought index sensitive to global warming: the standardized precipitation evapotranspiration index. *J. Climate* **23**, 1696–1718 (2010).
46. McKee, T. B., Doesken, N. J. & Kleist, J. The relationship of drought frequency and duration to time scales. *Eighth Conference on Applied Climatology, Anaheim, California, 17–22 January* (1993).
47. Milly, P. C. & Dunne, K. A. Potential evapotranspiration and continental drying. *Nat. Clim. Chang.* **6**, 946–949 (2016).
48. Berti, A., Tardivo, G., Chiaudani, A., Rech, F. & Borin, M. Assessing reference evapotranspiration by the hargreaves method in north-eastern Italy. *Agric. Water Manag.* **140**, 20–25 (2014).
49. Lasage, R. et al. A stepwise, participatory approach to design and implement community based adaptation to drought in the Peruvian Andes. *Sustainability* **7**, 1742–1773 (2015).
50. Yun, K.-S. et al. Increasing ENSO–rainfall variability due to changes in future tropical temperature–rainfall relationship. *Commun. Earth Environ.* **2**, 1–7 (2021).
51. Bury, J. T. et al. Glacier recession and human vulnerability in the Yanamarey watershed of the Cordillera Blanca, Peru. *Clim. Chang.* **105**, 179–206 (2011).
52. Polk, M. H. et al. Exploring hydrologic connections between tropical mountain wetlands and glacier recession in Peru's Cordillera Blanca. *Appl. Geogr.* **78**, 94–103 (2017).
53. Hagen, I. et al. Climate change-related risks and adaptation potential in Central and South America during the 21st century. *Environ. Res. Lett.* **17**, 033002 (2022).
54. Aparicio-Effen, M. et al. A successful early warning system for hydroclimatic extreme events: the case of la paz city mega landslide. *Climate Change Adaptation in Latin America: Managing Vulnerability, Fostering Resilience* 241–264 (2018).
55. Drenkhan, F., Huggel, C., Guardamino, L. & Haeberli, W. Managing risks and future options from new lakes in the deglaciating Andes of Peru: The example of the Vilcanota-Urubamba basin. *Sci. Total Environ.* **665**, 465–483 (2019).
56. Gesualdo, G. C., Oliveira, P. T., Rodrigues, D. B. B. & Gupta, H. V. Assessing water security in the São Paulo metropolitan region under projected climate change. *Hydrol. Earth Syst. Sci.* **23**, 4955–4968 (2019).
57. Barros, V. R. et al. Climate change in Argentina: trends, projections, impacts and adaptation. *Wiley Interdiscip. Rev. Clim. Chang.* **6**, 151–169 (2015).
58. Hannah, L. et al. Regional modeling of climate change impacts on smallholder agriculture and ecosystems in Central America. *Clim. Chang.* **141**, 29–45 (2017).
59. Huggel, C. et al. Glacier Lake 513, Peru: Lessons for early warning service development. *WMO Bull.* **69**, 45–52 (2020).
60. Rangecroft, S. et al. Climate change and water resources in arid mountains: an example from the Bolivian Andes. *Ambio* **42**, 852–863 (2013).
61. Skamarock, W. C. et al. A description of the advanced research WRF version 3 (Tech Rep). Tech. Rep., National Center For Atmospheric Research (2008).
62. Copernicus Climate Change Service (C3S) : ERA5: Fifth generation of ECMWF atmospheric reanalyses of the global climate. Copernicus Climate Change Service Climate Data Store (CDS) https://cds.climate.copernicus.eu/cdsapp#!/home (2017).
63. Hellström, R. Å et al. Incorporating autonomous sensors and climate modeling to gain insight into seasonal hydrometeorological processes within a tropical glacierized valley. *Ann. Am. Assoc. Geogr.* **107**, 260–273 (2017).
64. Posada-Marín, J. A., Rendón, A. M., Salazar, J. F., Mejía, J. F. & Villegas, J. C. WRF downscaling improves ERA-Interim representation of precipitation around a tropical Andean valley during El Niño: implications for GCM-scale simulation of precipitation over complex terrain. *Clim. Dyn.* **52**, 3609–3629 (2019).
65. Hunziker, S. et al. Identifying, attributing, and overcoming common data quality issues of manned station observations. *Int. J. Climatol.* **37**, 4131–4145 (2017).
66. Von Storch, H. & Zwiers, F. W.*Statistical Analysis in Climate Research* (Cambridge University Press, 2002).
67. Zhang, X. et al. Indices for monitoring changes in extremes based on daily temperature and precipitation data. *Wiley Interdiscip. Rev. Clim. Chang.* **2**, 851–870 (2011).
68. Logan, T. et al. Ouranosinc/xclim: v0.36.0 (2022). https://doi.org/10.5281/zenodo.6506567.
69. Hargreaves, G. H. & Samani, Z. A. Estimating potential evapotranspiration. *J. Irrigation Drainage Div.* **108**, 225–230 (1982).
70. Yevjevich, V. M. *Objective Approach to Definitions and Investigations of Continental Hydrologic Droughts,* Ph.D. thesis, Colorado State University. Libraries (1967).

ACKNOWLEDGEMENTS

This research was conducted under the Peru GROWS and PEGASUS projects, which were both funded by NERC (grants NE/S013296/1 and NE/S013318/1, respectively) and CONCYTEC through the Newton-Paulet Fund. The Peruvian part of the Peru GROWS project was conducted within the framework of the call E031-2018-01-NERC "Glacier Re-search Circles", through its executing unit FONDECYT (Contract No. 08-2019-FON-DECYT). We acknowledge the World Climate Research Programme's Working Group on Coupled Modeling, which is responsible for CMIP, and we thank the climate modeling groups (listed in Supplementary Table 7 of this paper) for producing and making available their model output. We thank SENAMHI, UNASAM, ANA, UNSAAC, and Compañia Minera Antamina for the observational data used in the historical bias correction, and we also thank Mario Rohrer at MeteoSwiss for assisting in data access. Thanks to J. Scott Hosking, Charles Simpson, Risa Ueno and Arthur Lutz for their advice on the statistical downscaling method. We acknowledge the Polar Data Centre for archiving the data used in this manuscript. This article is dedicated to the memory of Ing. Alejo Cochachin Rapre.

AUTHOR CONTRIBUTIONS

A.O., D.Q., A.R., S.R., E.P., C.F., H.B., A.L., G.J., R.H., J.C., E.L., and F.P. designed research; K.M, A.C., and N.M. provided observational data; E.P. and C.F. performed research, E.P. and C.F. analysed data, E.P., F.P., C.F., A.O., and S.R., wrote the paper with feedback from all authors.

COMPETING INTERESTS

The authors declare no competing interests.

ADDITIONAL INFORMATION

Supplementary information The online version contains supplementary material available at https://doi.org/10.1038/s41612-023-00409-z.

Correspondence and requests for materials should be addressed to Emily R. Potter.

Reprints and permission information is available at http://www.nature.com/reprints

Publisher's note Springer Nature remains neutral with regard to jurisdictional claims in published maps and institutional affiliations.